Model-Independent Analysis of the Orientation of Fluorescent Probes with Restricted Mobility in Muscle Fibers

R. E. Dale,* S. C. Hopkins,# U. A. an der Heide,# T. Marszałek,§ M. Irving,* and Y. E. Goldman#

*The Randall Institute, King's College London, London WC2B 5RL, England; #Pennsylvania Muscle Institute, The School of Medicine, University of Pennsylvania, Philadelphia, Pennsylvania 19104-6083; and §Institut Fizyki im. Aleksandra Jabłońskiego, Uniwersytet Mikołaja Kopernika, ul. Grudziądzka 5/7, 87-100 Toruń, Poland

ABSTRACT The orientation of proteins in ordered biological samples can be investigated using steady-state polarized fluorescence from probes conjugated to the protein. A general limitation of this approach is that the probes typically exhibit rapid orientational motion ("wobble") with respect to the protein backbone. Here we present a method for characterizing the extent of this wobble and for removing its effects from the available information about the static orientational distribution of the probes. The analysis depends on four assumptions: 1) the probe wobble is fast compared with the nanosecond time scale of its excited-state decay; 2) the orientational distributions of the absorption and emission transition dipole moments are cylindrically symmetrical about a common axis *c* fixed in the protein; 3) protein motions are negligible during the excited-state decay; 4) the distribution of *c* is cylindrically symmetrical about the director of the experimental sample. In a muscle fiber, the director is the fiber axis, *F*. All of the information on the orientational order of the probe that is available from measurements of linearly polarized fluorescence is contained in five independent polarized fluorescence intensities measured with excitation and emission polarizers parallel or perpendicular to *F* and with the propagation axis of the detected fluorescence parallel or perpendicular to that of the excitation. The analysis then yields the average second-rank and fourth-rank order parameters ($\langle P_2 \rangle$ and $\langle P_4 \rangle$) of the angular distribution of *c* relative to *F*, and $\langle P_{2a} \rangle$ and $\langle P_{2e} \rangle$, the average second-rank order parameters of the angular distribution for wobble of the absorption and emission transition dipole moments relative to *c*. The method can also be applied to other cylindrically ordered systems such as oriented lipid bilayer membranes and to processes slower than fluorescence that may be observed using longer-lived optically excited states.

INTRODUCTION

Intrinsic and extrinsic luminescent (fluorescent and phosphorescent) probes have been highly successful tools in investigations of the orientation of the components of macromolecular and supramolecular structures. Steady-state and time-resolved measurements of polarized luminescence have revealed rotational motions in these systems over a range of time scales from nanoseconds to milliseconds (see, e.g., Munro et al., 1979; Jovin et al., 1981). In these studies, it is necessary to distinguish the local orientational distribution and motions of the reporter groups relative to the macromolecules from those of the macromolecules themselves, which are usually more functionally relevant. The intrinsic protein fluorophore tryptophan, for instance, exhibits restricted orientational motion with respect to the protein frame (Beechem and Brand, 1985). Extrinsic probes that are covalently bound to proteins also rotate around their linkers and wobble within restricted angular ranges on the subnanosecond time scale (Brochon et al., 1972; Wahl et al., 1978). The segmental flexibility of neighboring peptide regions leads to similar restricted probe rotations on somewhat longer time scales (Yguerabide et al., 1970). Such local motions depolarize the emission from the probes and must be taken into account when fluorescence polarization is used to analyze protein orientation and motion. Local probe motions are usually sufficiently restricted that they do not obscure information about the orientation of the protein.

The rate and extent of restricted probe rotations in supramolecular structures, which occur on the nanosecond or subnanosecond time scale, are usually determined from the decay of fluorescence anisotropy (see, e.g., Munro et al., 1979), using isotropic samples, for example, suspensions of myofibrils (Ishiwata et al., 1987; Ludescher and Thomas, 1988) or myosin synthetic filaments (Kinosita et al., 1984). However, there are several potential problems with this approach. Preparation of soluble or suspendable components of the sample and maintenance of an isotropic orientation are not always straightforward. Critically, the measured properties of the isotropic sample, including the angular probe mobility, may be different from those in the native, fully constituted system. Techniques for measuring nanosecond anisotropy decays are relatively complex, requiring specialized apparatus and, usually, long data acquisition times (Badea and Brand, 1979; Lakowicz and Maliwal, 1985), limiting their usefulness for dynamic or unstable supramolecular systems.

An ordered sample is required to characterize orientational distributions relative to a symmetry axis in the system. It has been shown previously that dynamics can also be characterized in ordered systems by polarized fluorescence experiments without the need for nanosecond time-resolved equipment (Kooyman et al., 1981, 1983). These measurements can be made using static polarizers in the excitation

Received for publication 23 July 1998 and in final form 11 December 1998.

Address reprint requests to Dr. Yale E. Goldman, Department of Physiology, University of Pennsylvania School of Medicine, D701 Richards Building, 3700 Hamilton Walk, Philadelphia, PA 19104-6083. Tel.: 215-898-4017; Fax: 215-898-2653; E-mail: goldmany@mail.med.upenn.edu.

0006-3495/99/03/1606/13 $2.00

and emission channels (e.g., Van Gurp et al., 1988a,b; Ling et al., 1996) or electronically modulated polarizers, allowing repeated measurements at submillisecond intervals if light levels are sufficiently high (Irving et al., 1995; Allen et al., 1996; Hopkins et al., 1998). Compared to nanosecond time-resolved experiments, these methods offer convenience and speed at the expense of more limited resolution of the rotational dynamics.

In many cases the underlying distribution of protein orientations, rather than the detailed behavior of the probe relative to the protein, is the primary interest. A useful analytical framework for interpreting fluorescence polarization measurements in cylindrically symmetrical systems has been presented by Irving (1996). Equations for polarized intensities in an ordered system, such as a muscle fiber, were formulated to separate the effects of very rapid probe wobble, considered to be restricted within a cone centered on a stationary axis in the sample. With these equations, fluorescence polarization data obtained from muscle fibers during physiological events could be quantitatively interpreted by modeling the orientational distribution of the cone axis (e.g., Allen et al., 1996; Ling et al., 1996; Hopkins et al., 1998). However, the specific choice of the model orientational distribution (e.g., a Gaussian) often affected the results, thereby limiting the conclusions that could be drawn. A more general analysis, not requiring the selection of model distributions, would thus be advantageous.

In the present report, we show that, with several reasonable assumptions about the characteristics of the local probe motions, it is possible to take these into account without adopting a specific form for either the static orientational distribution or the motions of the probes. These basic assumptions are 1) the restricted motions ("wobble") of the probes with respect to the protein frame are fast relative to the decay of the optically excited state; 2) the orientational distributions of the absorption and emission transition dipole moments are cylindrically symmetrical about an axis, *c*, and the orientations relative to *c* are independent of the orientation of *c* in the ordered system; 3) *c* is fixed within the protein, and protein reorientation is negligible on the time scale of decay of the optically excited state; 4) the ordered system under study has overall cylindrical symmetry.

The amplitude of the rapid wobble is characterized by the two second-rank order parameters $\langle P_{2a}\rangle$ and $\langle P_{2e}\rangle$ for the absorption and emission transition dipole moments (*a* and *e*, respectively) when they are not colinear, or by a single order parameter $\langle P_{2d}\rangle$ when *a* and *e* are colinear. Other than the condition embodied in assumption 1, the analysis does not provide an estimate of the rate of this wobble. More importantly, the analysis yields estimates of the second-rank and fourth-rank order parameters ($\langle P_2\rangle$ and $\langle P_4\rangle$) describing the static distribution of *c* relative to the symmetry axis, free of the effects of the wobble. Changes in the orientational distribution of *c* between different functional states, as reflected in $\langle P_2\rangle$ and $\langle P_4\rangle$, may reveal structural and mechanistic features of the system under study. The analysis is described here for the example of a muscle fiber, but it is also relevant to other ordered assemblies with effective cylindrical symmetry, such as planar lipid bilayer membranes, and to rotational events monitored on the longer time scale of triplet excited-state decay. Part of this work has previously been presented in abstract form (Dale et al., 1997).

THEORY

The analysis is developed for the example of a muscle fiber containing fluorophores bound at a specific site on a protein. The inherent symmetries of the muscle filament lattice and the azimuthally random orientations of the constituent myofibrils impose effective cylindrical symmetry about the muscle fiber axis *F* (the sample director). The common average orientation of the absorption and emission transition dipole moments, *a* and *e*, of the probe (or that of the common transition dipole moment *d* when they are colinear) defines an axis, *c*, fixed within the labeled protein. The distributions of *a* and *e*, or of *d*, are assumed to be cylindrically symmetrical about *c*. The orientational distribution of *c* relative to *F* is not specified, except that it is also cylindrically symmetrical. Rotational correlation times for motions of the protein within the muscle fiber are assumed to be on the microsecond to millisecond time scale, much longer than the fluorescence lifetime (see, e.g., Kinosita et al., 1984; Ishiwata et al., 1987; Ludescher and Thomas, 1988; Stein et al., 1990). Thus, on the nanosecond time scale of fluorescence, the protein orientational distribution, and therefore that of *c*, is treated as effectively static.

In the following, we show that, under assumptions 1–4 listed in the Introduction, the effect of fast motions of the absorption and emission transition dipole moments can be factored out from the parameters describing the static orientation of *c*. In the simplest case, the transition dipole moments for absorption and emission are colinear within the framework of the probe ($a \parallel e \equiv d$), and three independent polarization ratios (four independent polarized intensities) can be measured. The condition of dipole-moment colinearity is reasonably well met for the longest-wavelength strong absorption transition in many fluorophores. The colinearity assumption can be relaxed, provided that the distributions of the two transition dipole moments are cylindrically symmetrical about the same axis, *c* (condition 2 in the Introduction). It is then necessary to determine a fourth independent polarization ratio (or fifth polarized intensity). This more general case will be developed first, and the reduced result for colinear transition dipole moments will be derived from it.

Legendre polynomial representation of orientational distributions

Let $f(\beta_{Fc})$ be the orientational distribution of *c* relative to the fiber axis *F*, normalized such that $\int_0^\pi f(\beta_{Fc})\sin\beta_{Fc}\, d\beta_{Fc} = 1$. Then $f(\beta_{Fc})$ can be approximated to an arbitrary fidelity

(depending on the number of terms, N) by an expansion of the form

$$f(\beta_{Fc}) \cong \sum_{j=0}^{N} \frac{2j+1}{2} \langle P_j \rangle P_j(\cos \beta_{Fc}) \quad (1)$$

(Zannoni, 1988), where $P_j(z)$ is the jth Legendre polynomial, e.g., $P_0(z) = 1$, $P_1(z) = z$, $P_2(z) = (3z^2 - 1)/2$, $P_3(z) = (5z^3 - 3z)/2$, $P_4(z) = (35z^4 - 30z^2 + 3)/8$, etc., and $\langle P_j \rangle$ is the average value of $P_j(\cos \beta_{Fc})$ over the normalized distribution $f(\beta_{Fc})$:

$$\langle P_j \rangle = \int_0^{\pi} P_j(\cos \beta_{Fc}) f(\beta_{Fc}) \sin \beta_{Fc} \, d\beta_{Fc} \quad j = [0, N]. \quad (2)$$

The Legendre polynomials P_j form a set of orthogonal basis functions. An exact description of the orientational distribution of the probe is provided by the infinite set of these functions in the expansion of Eq. 1. The average values, $\langle P_j \rangle$, of these functions over the distribution (Eq. 2), which are the scaling coefficients for the terms in Eq. 1, are known as the order parameters of the distribution.

The probes are bound to a specific site on the protein that determines their orientation relative to the protein coordinates. They are assumed to rotate rapidly (wobble) over a limited range in such a way that the orientational distribution of the absorption and emission transition dipole moments is cylindrically symmetrical about c. The amplitude of this restricted rotation is characterized by its second-rank order parameter, for example, $\langle P_{2a} \rangle \equiv \langle P_2(\cos \beta_{ca}) \rangle = (3\langle \cos^2 \beta_{ca} \rangle - 1)/2$, where β_{ca} is the instantaneous angle between the mobile transition dipole moment a and the stationary axis c. Starting from an appropriate set of fluorescence polarization measurements, the analysis presented here yields estimates of $\langle P_{2a} \rangle$ and $\langle P_{2e} \rangle$ (or $\langle P_{2d} \rangle$ if the dipole moments are colinear) for the rapid wobble and the second- and fourth-rank order parameters, $\langle P_2 \rangle \equiv \langle P_2(\cos \beta_{Fc}) \rangle$ and $\langle P_4 \rangle \equiv \langle P_4(\cos \beta_{Fc}) \rangle$, of the orientational distribution of c relative to F.

Polarized fluorescence

The geometry for excitation and observation of polarized components of fluorescence from an ensemble of probe molecules in a muscle fiber is illustrated in Fig. 1. The fiber axis F is oriented along the z-axis of the laboratory coordinate system. The absorption and emission transition dipole moments of the probe are designated by the unit vectors a and e, respectively. The observed intensity of linearly polarized fluorescence, ${}_{E}I_{E'}$, where E and E' are vectors denoting the orientation of polarizers in the paths of the exciting and emitted beams, depends on the orientations of a and e, the intensity of the excitation, the gain of the detection system, the quantum efficiency of fluorescence, and the effective fluorophore concentration. All of these factors except the orientation dependence are taken up in a scaling intensity (I). The polarized intensity ${}_{E}I_{E'}$ is then given by

$${}_{E}I_{E'} = I\langle (E \cdot a)^2 (E' \cdot e)^2 \rangle = I\langle \cos^2 \beta_{Ea} \cos^2 \beta_{E'e} \rangle, \quad (3)$$

in which the brackets $\langle \, \rangle$ indicate averaging over the ensemble of probe molecules and over the time course of the excited-state decay. The separation of the effects of very rapid restricted rotations from those of static order under the present set of assumptions is outlined below. A detailed derivation in terms of simple trigonometric functions is given in Appendix A, and a more general treatment, formulated in terms of Wigner rotation matrices, appears in Appendix B.

The effects of rapid restricted rotation are conveniently separated out before the details of the static orientational

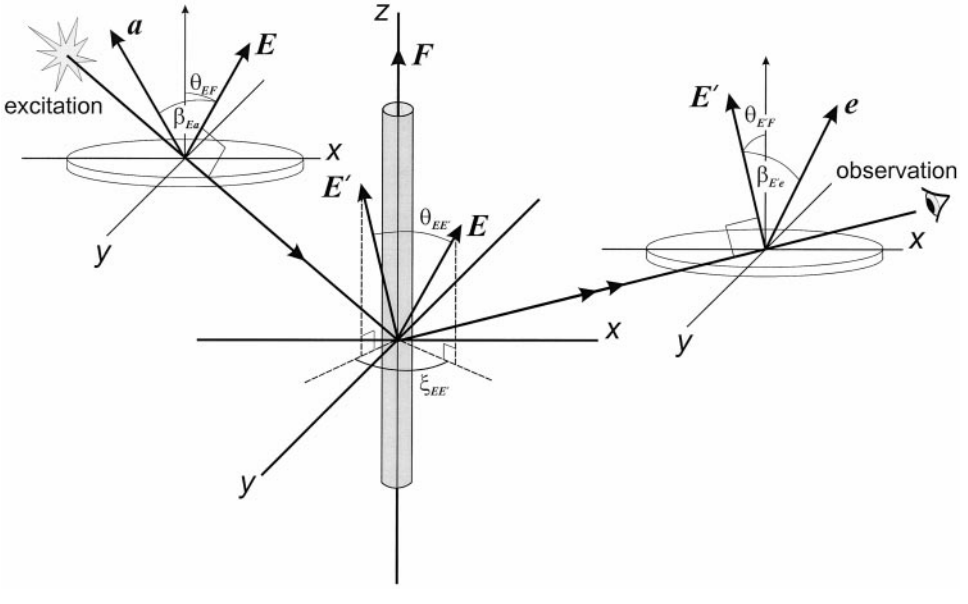

FIGURE 1 Experimental geometry for excitation (→) and observation (→→) of a fluorescently labeled muscle fiber. Axis F is aligned along the laboratory z axis, with electric vectors E and E' for exciting and emitted light, respectively. The absorption and emission transition dipole moments are a and e, respectively. The projections of E and E' onto the xy plane, perpendicular to F, subtend an azimuth $\xi_{EE'}$.

distribution are considered. Equation 3 is first recast in the form of second-rank Legendre polynomials (Van der Meer et al., 1982):

$$ {}_{\mathrm{E}}I_{\mathrm{E}'} = \frac{I}{9}[1 + 2\langle P_2(\cos\beta_{\mathrm{Ea}})\rangle + 2\langle P_2(\cos\beta_{\mathrm{E}'e})\rangle + 4\langle P_2(\cos\beta_{\mathrm{Ea}})P_2(\cos\beta_{\mathrm{E}'e})\rangle], \tag{4} $$

where all of the angle brackets denote averaging over the ensemble of probe molecules, but those around the product term also imply time averaging over the decay of the excited state. No assumptions are made about the symmetry of the system in obtaining Eq. 4.

At the instant of excitation, *a* and *e* are correlated (even if they are not colinear). If the restricted rotation is fast compared to the decay of the excited state, all "memory" of the probe orientation (within its restricted range) at the instant of excitation is lost before the instant of emission. Thus the orientation of *e*, within its restricted range, at emission is independent of the orientation of *a*, within its restricted range, at excitation. If the distributions of *a* and *e* are cylindrically symmetrical about a unique axis *c* in the frame of the protein to which the probe is attached, then, as shown in Appendices A and B (Eqs. A2, A4, A5, and B16–B18), the averaged second-rank order parameters in Eq. 4 can be expressed as the products of those for the orientations of *a* and *e* with respect to *c* and those for the orientation of *c* with respect to *E* and *E′*, respectively, leading to

$$ {}_{\mathrm{E}}I_{\mathrm{E}'} = \frac{I}{9}[1 + 2\langle P_{2\mathrm{a}}\rangle\langle P_2(\cos\beta_{\mathrm{Ec}})\rangle + 2\langle P_{2\mathrm{e}}\rangle\langle P_2(\cos\beta_{\mathrm{E}'c})\rangle + 4\langle P_{2\mathrm{a}}\rangle\langle P_{2\mathrm{e}}\rangle\langle P_2(\cos\beta_{\mathrm{Ec}})P_2(\cos\beta_{\mathrm{E}'c})\rangle]. \tag{5} $$

This result is still independent of any symmetry of the orientational distribution of *c*. However, if the distribution of *c* is now assumed to be cylindrically symmetrical about *F*, the terms $\langle P_2(\cos\beta_{\mathrm{Ec}})\rangle$ and $\langle P_2(\cos\beta_{\mathrm{E}'c})\rangle$ appearing in Eq. 5 factorize into $P_2(\cos\theta_{\mathrm{EF}})\,\langle P_2(\cos\beta_{\mathrm{Fc}})\rangle$ and $P_2(\cos\theta_{\mathrm{E}'\mathrm{F}})\,\langle P_2(\cos\beta_{\mathrm{Fc}})\rangle$, respectively, as also detailed in Appendices A and B (Eqs. A8–A9, and B26–B27), thus separating the parameters related to the experimental geometry from those describing the orientational distribution of the sample.

$P_2(\cos\beta_{\mathrm{Ec}})$ and $P_2(\cos\beta_{\mathrm{E}'c})$ also appear as the average of their product in the fourth term in Eq. 5. This average depends on the correlation between β_{Ec} at the instant of excitation and $\beta_{\mathrm{E}'c}$ at the instant of emission. The condition that *c* is stationary over this time period (condition 3 in the Introduction) is now introduced. Averaging this product over the azimuthal distributions leads to three terms, in which parameters related to the experimental geometry are again separated from those describing the orientational distribution of the sample (Appendices A and B, Eqs. A12 and B31).

The final result for ${}_{\mathrm{E}}I_{\mathrm{E}'}$ may be expressed in the form given by Van der Meer et al. (1982):

$$ \begin{aligned} {}_{\mathrm{E}}I_{\mathrm{E}'} = \frac{I}{9}[&1 + (3\cos^2\theta_{\mathrm{EF}} - 1)S_{\mathrm{a}} + (3\cos^2\theta_{\mathrm{E}'\mathrm{F}} - 1)S_{\mathrm{e}} \\ &+ (3\cos^2\theta_{\mathrm{EF}} - 1)(3\cos^2\theta_{\mathrm{E}'\mathrm{F}} - 1)G_0 \\ &+ (3\sin 2\theta_{\mathrm{EF}}\sin 2\theta_{\mathrm{E}'\mathrm{F}}\cos\xi_{\mathrm{EE}'})G_1 \\ &+ (3\sin^2\theta_{\mathrm{EF}}\sin^2\theta_{\mathrm{E}'\mathrm{F}}\cos 2\xi_{\mathrm{EE}'})G_2], \end{aligned} \tag{6} $$

in which the parameters related to the experimental geometry, θ_{EF}, $\theta_{\mathrm{E}'\mathrm{F}}$ and their azimuth $\xi_{\mathrm{EE}'}$ in the plane perpendicular to *F* are defined in Fig. 1. S_{a} and S_{e} are the second-rank order parameters for *a* and *e* with respect to the fiber axis *F*, and the G_{i} are correlation functions for *a* and *e* with respect to *F*, and are defined by

$$ S_{\mathrm{a}} = \langle P_{2\mathrm{a}}\rangle\langle P_2\rangle \tag{7} $$

$$ S_{\mathrm{e}} = \langle P_{2\mathrm{e}}\rangle\langle P_2\rangle \tag{8} $$

$$ \begin{aligned} G_0 &= \langle P_{2\mathrm{a}}\rangle\langle P_{2\mathrm{e}}\rangle\langle P_2^2(\cos\beta_{\mathrm{Fc}})\rangle \\ &= \langle P_{2\mathrm{a}}\rangle\langle P_{2\mathrm{e}}\rangle\left(\frac{1}{5} + \frac{2}{7}\langle P_2\rangle + \frac{18}{35}\langle P_4\rangle\right) \end{aligned} \tag{9} $$

$$ \begin{aligned} G_1 &= \langle P_{2\mathrm{a}}\rangle\langle P_{2\mathrm{e}}\rangle\left\langle\frac{3}{8}\sin^2 2\beta_{\mathrm{Fc}}\right\rangle \\ &= \langle P_{2\mathrm{a}}\rangle\langle P_{2\mathrm{e}}\rangle\left(\frac{1}{5} + \frac{1}{7}\langle P_2\rangle - \frac{12}{35}\langle P_4\rangle\right) \end{aligned} \tag{10} $$

$$ \begin{aligned} G_2 &= \langle P_{2\mathrm{a}}\rangle\langle P_{2\mathrm{e}}\rangle\left\langle\frac{3}{8}\sin^4\beta_{\mathrm{Fc}}\right\rangle \\ &= \langle P_{2\mathrm{a}}\rangle\langle P_{2\mathrm{e}}\rangle\left(\frac{1}{5} - \frac{2}{7}\langle P_2\rangle + \frac{3}{35}\langle P_4\rangle\right), \end{aligned} \tag{11} $$

where $\langle P_2\rangle \equiv \langle P_2(\cos\beta_{\mathrm{Fc}})\rangle$ and $\langle P_4\rangle \equiv \langle P_4(\cos\beta_{\mathrm{Fc}})\rangle$.

In practice, only S_{a}, S_{e}, G_0, and G_2 are determined experimentally. However, from Eqs. 9–11, the G_{i} are related by

$$ G_0 + 2(G_1 + G_2) = \langle P_{2\mathrm{a}}\rangle\langle P_{2\mathrm{e}}\rangle, \tag{12} $$

so that only two of them are independent. This is useful because, as discussed in the Experimental Section, direct measurement of G_1 is not straightforward in highly birefringent samples like muscle fibers. Thus, in practice, the four independent order parameters $\langle P_{2\mathrm{a}}\rangle$, $\langle P_{2\mathrm{e}}\rangle$, $\langle P_2\rangle$, and $\langle P_4\rangle$ are obtained by inversion of Eqs. 7–9 and 11:

$$ \langle P_{2\mathrm{a}}\rangle = S_{\mathrm{a}}\left(1 + \sqrt{1 + \frac{6G_2 - G_0}{S_{\mathrm{a}}S_{\mathrm{e}}}}\right) \tag{13} $$

$$ \langle P_{2\mathrm{e}}\rangle = S_{\mathrm{e}}\left(1 + \sqrt{1 + \frac{6G_2 - G_0}{S_{\mathrm{a}}S_{\mathrm{e}}}}\right) \tag{14} $$

$$ \langle P_2\rangle = \frac{S_{\mathrm{a}}}{\langle P_{2\mathrm{a}}\rangle} = \frac{S_{\mathrm{e}}}{\langle P_{2\mathrm{e}}\rangle} \tag{15} $$

$$\langle P_4\rangle = \frac{5}{3}\left(\frac{G_0 + G_2}{\langle P_{2a}\rangle\langle P_{2e}\rangle}\right) - \frac{2}{3}. \quad (16)$$

When a and e are colinear, and the orientational distributions of the rapid local wobble are identical for the ground and excited states, $\langle P_{2d}\rangle$ can be substituted for both $\langle P_{2a}\rangle$ and $\langle P_{2e}\rangle$ in Eqs. 5 and 7–16 above. Then $S_a = S_e \equiv S_d$ and Eqs. 13 and 14 reduce to

$$\langle P_{2d}\rangle = S_d + \sqrt{S_d^2 + 6G_2 - G_0}. \quad (17)$$

EXPERIMENTAL CONSIDERATIONS

In the previous section, it was shown how the order parameters for the static part of the distribution of the probes in the sample are obtained from S_a, S_e, G_0, and G_2, free of the effects of rapid probe motion. In this section, it is shown how S_a, S_e, G_0, and G_2 are obtained from the polarized intensities or polarization ratios measured experimentally.

The experimental geometries commonly used in fluorescence polarization experiments on oriented samples like muscle fibers are the epifluorescence or upright fluorescence microscope, with 0° or 180° between the propagation axes of the exciting and observed beams (i.e., in-line, x-illumination) and the T-format or L-format (spectro)fluorimeter, with 90° between the propagation axes (right-angle, y-illumination). Hopkins et al. (1998) have described a T-format system usefully combining both in-line and right-angle illumination. In these geometries, all of the available information about the orientational distribution of samples with the symmetries and motional time regimes considered here can be obtained from five independent polarized fluorescence intensities ($_{E}I_{E'}$) measured with exciting and emitted beams polarized parallel or perpendicular to the sample director F, the fiber axis. These are $_{\parallel}I_{\parallel}$, $_{\parallel}I_{\perp}$, and $_{\perp}I_{\parallel}$, the values of which are the same in the x- and y-illumination geometries, $^{x}_{\perp}I_{\perp}$ ($\xi_{EE'} = 0$ or π; Fig. 1) and $^{y}_{\perp}I_{\perp}$ ($\xi_{EE'} = \pi/2$). Substitution of $\theta_{EF} = 0$, $\theta_{E'F} = 0$ for parallel polarizations, and $\theta_{EF} = \pi/2$, $\theta_{E'F} = \pi/2$ for perpendicular polarizations, into Eq. 6 gives

$$_{\parallel}I_{\parallel} = \frac{I}{9}(1 + 2S_a + 2S_e + 4G_0) \quad (18)$$

$$_{\parallel}I_{\perp} = \frac{I}{9}(1 + 2S_a - S_e - 2G_0) \quad (19)$$

$$_{\perp}I_{\parallel} = \frac{I}{9}(1 - S_a + 2S_e - 2G_0) \quad (20)$$

$$^{x}_{\perp}I_{\perp} = \frac{I}{9}(1 - S_a - S_e + G_0 + 3G_2) \quad (21)$$

$$^{y}_{\perp}I_{\perp} = \frac{I}{9}(1 - S_a - S_e + G_0 - 3G_2) \quad (22)$$

(see also Van Gurp et al., 1988a; Van der Heide et al., 1994). G_1 does not appear in these relationships, because of the choice of x- and y-illumination together with parallel and perpendicular polarizations. However, G_1 gives no extra information about probe orientation under the assumptions made in the present analysis, as already discussed (Eq. 12).

Equations 18–22 can be inverted to give expressions for S_a, S_e, G_0, G_2 and the total intensity, I, in terms of the polarized intensities:

$$S_a = 1 - \frac{3}{I}(_{\perp}I_{\parallel} + ^{x}_{\perp}I_{\perp} + ^{y}_{\perp}I_{\perp}) \quad (23)$$

$$S_e = 1 - \frac{3}{I}(_{\parallel}I_{\perp} + ^{x}_{\perp}I_{\perp} + ^{y}_{\perp}I_{\perp}) \quad (24)$$

$$G_0 = \frac{3}{2I}(_{\parallel}I_{\parallel} + ^{x}_{\perp}I_{\perp} + ^{y}_{\perp}I_{\perp}) - \frac{1}{2} \quad (25)$$

$$G_2 = \frac{3}{2I}(^{x}_{\perp}I_{\perp} - ^{y}_{\perp}I_{\perp}) \quad (26)$$

$$I = _{\parallel}I_{\parallel} + 2(_{\perp}I_{\parallel} + _{\parallel}I_{\perp} + ^{x}_{\perp}I_{\perp} + ^{y}_{\perp}I_{\perp}). \quad (27)$$

Experimentally, relative polarized fluorescence intensities are often derived from direct measurements of polarization ratios (classically, degree of polarization, or simply polarization), which are independent of the absolute fluorescence intensity (e.g., Tregear and Mendelson, 1975; Irving et al., 1995; Hopkins et al., 1998). The polarization ratios commonly used are

$$Q_{\parallel} = (_{\parallel}I_{\parallel} - _{\perp}I_{\parallel})/(_{\parallel}I_{\parallel} + _{\perp}I_{\parallel}) \quad (28)$$

$$^{x}Q_{\perp} = (^{x}_{\perp}I_{\perp} - _{\parallel}I_{\perp})/(^{x}_{\perp}I_{\perp} + _{\parallel}I_{\perp}) \quad (29)$$

$$^{y}Q_{\perp} = (^{y}_{\perp}I_{\perp} - _{\parallel}I_{\perp})/(^{y}_{\perp}I_{\perp} + _{\parallel}I_{\perp}) \quad (30)$$

and

$$P_{\parallel} = (_{\parallel}I_{\parallel} - _{\parallel}I_{\perp})/(_{\parallel}I_{\parallel} + _{\parallel}I_{\perp}) \quad (31)$$

$$^{x}P_{\perp} = (^{x}_{\perp}I_{\perp} - _{\perp}I_{\parallel})/(^{x}_{\perp}I_{\perp} + _{\perp}I_{\parallel}) \quad (32)$$

$$^{y}P_{\perp} = (^{y}_{\perp}I_{\perp} - _{\perp}I_{\parallel})/(^{y}_{\perp}I_{\perp} + _{\perp}I_{\parallel}). \quad (33)$$

Polarized intensities relative to a chosen reference intensity are obtained by inversion of Eqs. 28–33. For example, using $_{\parallel}I_{\parallel}$ as the reference intensity, these are

$$_{\perp}R_{\parallel} = \frac{_{\perp}I_{\parallel}}{_{\parallel}I_{\parallel}} = \frac{1 - Q_{\parallel}}{1 + Q_{\parallel}} \quad (34)$$

$$_{\parallel}R_{\perp} = \frac{_{\parallel}I_{\perp}}{_{\parallel}I_{\parallel}} = \frac{1 - P_{\parallel}}{1 + P_{\parallel}} \quad (35)$$

$$^{x}_{\perp}R_{\perp} = \frac{^{x}_{\perp}I_{\perp}}{_{\parallel}I_{\parallel}} = \left(\frac{1 + ^{x}Q_{\perp}}{1 - ^{x}Q_{\perp}}\right)\left(\frac{1 - P_{\parallel}}{1 + P_{\parallel}}\right) = \left(\frac{1 + ^{x}P_{\perp}}{1 - ^{x}P_{\perp}}\right)\left(\frac{1 - Q_{\parallel}}{1 + Q_{\parallel}}\right) \quad (36)$$

$$^{y}_{\perp}R_{\perp} = \frac{^{y}_{\perp}I_{\perp}}{_{\parallel}I_{\parallel}} = \left(\frac{1 + ^{y}Q_{\perp}}{1 - ^{y}Q_{\perp}}\right)\left(\frac{1 - P_{\parallel}}{1 + P_{\parallel}}\right) = \left(\frac{1 + ^{y}P_{\perp}}{1 - ^{y}P_{\perp}}\right)\left(\frac{1 - Q_{\parallel}}{1 + Q_{\parallel}}\right). \quad (37)$$

On defining $R = (I/{}_{\|}I_{\|}) = 1 + 2({}_{\perp}R_{\|} + {}_{\|}R_{\perp} + {}^{x}_{\perp}R_{\perp} + {}^{y}_{\perp}R_{\perp})$, the order parameters and correlation functions S_a, S_e, G_0, and G_2 are obtained as

$$S_a = 1 - \frac{3}{R}({}_{\perp}R_{\|} + {}^{x}_{\perp}R_{\perp} + {}^{y}_{\perp}R_{\perp}) \quad (38)$$

$$S_e = 1 - \frac{3}{R}({}_{\|}R_{\perp} + {}^{x}_{\perp}R_{\perp} + {}^{y}_{\perp}R_{\perp}) \quad (39)$$

$$G_0 = \frac{3}{2R}(1 + {}^{x}_{\perp}R_{\perp} + {}^{y}_{\perp}R_{\perp}) - \frac{1}{2} \quad (40)$$

$$G_2 = \frac{3}{2R}({}^{x}_{\perp}R_{\perp} - {}^{y}_{\perp}R_{\perp}). \quad (41)$$

Using Eqs. 34–41, S_a, S_e, G_0, and G_2 can thus be calculated from the experimentally determined polarization ratios Q and P. Equations 13–16 are then used to calculate $\langle P_2\rangle$, $\langle P_4\rangle$, $\langle P_{2a}\rangle$, and $\langle P_{2e}\rangle$. If the absorption and emission transition dipole moments are colinear and the orientational distributions of the rapid wobble are identical in the ground and excited states, ${}_{\perp}I_{\|} = {}_{\|}I_{\perp}$, and each polarization ratio P is equal to the corresponding ratio Q, so that either set may be used in Eqs. 34–37, and ${}_{\perp}R_{\|} = {}_{\|}R_{\perp}$, $S_a = S_e \equiv S_d$. The analysis then yields $\langle P_2\rangle$, $\langle P_4\rangle$, and $\langle P_{2d}\rangle$.

DISCUSSION

We have described a simple method for analyzing and interpreting data from fluorescence polarization experiments on cylindrically symmetrical ordered samples. The results yield estimates of the second-rank and fourth-rank order parameters, $\langle P_2\rangle$ and $\langle P_4\rangle$, for c, the static part of the orientational distribution of the fluorophore, with respect to the sample director F. Estimates of the second-rank order parameters $\langle P_{2a}\rangle$ and $\langle P_{2e}\rangle$ characterizing the extent of rapid wobble of the absorption and emission transition dipole moments of the probe around c are also obtained. This method characterizes the static part of the orientational distribution of the fluorophore, while avoiding detailed modeling of its rapid restricted wobble. An additional advantage of this approach over model-based analyses is that it provides a unique mapping from four linearly independent observed quantities, e.g., the fluorescence polarization ratios $Q_{\|}$, $P_{\|}$, ${}^{x}Q_{\perp}$, and ${}^{y}Q_{\perp}$, to the four extracted parameters, $\langle P_2\rangle$, $\langle P_4\rangle$, $\langle P_{2a}\rangle$, and $\langle P_{2e}\rangle$, using all of the experimentally accessible information. There is no restriction on the form of the static orientational distribution of c, other than that it is cylindrically symmetrical about the director (fiber axis).

Colinear transition dipole moments

The absorption and emission transition dipole moments (a and e) can often be considered to be colinear. This holds at least approximately when these involve the same electronic levels, e.g., for fluorescence and the strong, longest wavelength absorption in xanthene-derivative fluorophores like rhodamine and fluorescein (Chen and Bowman, 1965), the transition dipole moments being closely aligned with the long axis of the xanthene conjugated-ring system (Penzkofer and Wiedmann, 1980). However, recent experimental evidence indicates that these transition dipole moments in eosin, another xanthene derivative, may not be colinear (Van der Heide et al., 1992b).

It is also usually assumed that the equilibrium ground- and excited-state molecular orientational distributions are identical, but because the ground and excited states are chemically and physically distinct, this assumption may not be valid (Razi Naqvi, 1981). Nonequivalence of these distributions provides a possible alternative explanation for differing experimental values of S_a and S_e, with fluorophores nominally having colinear absorption and emission transition moments (Johansson, 1985; Mulders et al., 1986). Under the assumptions made in the present analysis, the effects of differing ground- and excited-state orientational distributions are not distinguishable from those of fast rotation of noncolinear transition dipoles a and e about the same axis c.

In the case of colinear transition dipole moments behaving identically in ground and excited states, the method generates $\langle P_2\rangle$, $\langle P_4\rangle$, and $\langle P_{2d}\rangle$, the shared second-rank order parameter for the orientational distribution of the restricted probe wobble, from three linearly independent observables, e.g., the three Q polarization ratios.

Symmetry considerations

The present analysis can be applied to cylindrically symmetrical systems such as oriented muscle fibers, where the symmetry axis (sample director) is the axis of the fiber, and oriented lipid membranes, where the sample director is the normal to the plane of the membrane. The approach is also valid for ordered samples with five-fold or greater azimuthal symmetry around the sample director. This criterion is met in individual myosin filaments of vertebrate striated muscle, which have ninefold azimuthal symmetry. Moreover, in a muscle fiber, the random azimuthal orientations of the constituent myofibrils ensure effective cylindrical symmetry. In lipid membranes, random azimuthal orientation is ensured by the absence of long-range order in the plane of the membrane.

Cylindrically symmetrical samples often exhibit additional symmetry about the plane perpendicular to the director. Muscle sarcomeres and whole fibers exhibit twofold rotational symmetry about this plane. Probes attached asymmetrically to components of bilayer membranes are also twofold symmetrical about the plane of the membrane, whereas mirror symmetry across this plane is typical for probes dissolved directly in the lipid bilayer. These symmetries are compatible with the analysis developed here, but they are not required, and the analysis is also valid for systems without twofold or mirror symmetry, such as single half-sarcomeres or lipid monolayers.

Time regimes for probe and protein rotations

The difference in size between the protein and the attached fluorophore typically leads to rotational diffusion on very different time scales. The correlation time, φ, for rotational diffusion of a spherical protein in solution is given approximately by $\eta V/RT$, where η is the effective viscosity of the medium, V is the molar volume of the hydrated protein, R is the gas constant, and T is the absolute temperature (Lakowicz, 1983). Thus, in a dilute aqueous buffer at room temperature, a compact globular protein the size of myosin subfragment 1 (S-1, molecular mass ~130 kDa) would be expected to exhibit a rotational correlation time of ~60 ns. Correlation times for axial rotation can be appreciably greater if the macromolecule is elongated. For example, myosin S-1 has a length-to-width ratio of ~4:1 and exhibits average rotational correlation times of ~200 ns in aqueous solutions (Mendelson et al., 1973; Van der Heide et al., 1992a). The protein may also be in a viscous or anisotropic medium or integrated into a larger ordered structure, which would limit and slow its rotation. In these situations, the observed correlation times can extend into the microsecond and even millisecond time ranges, as in isolated myofibrils (Ishiwata et al., 1987; Ludescher and Thomas, 1988) or muscle fiber bundles (Stein et al., 1990).

On the other hand, free probes with molecular masses of only a few hundred daltons typically have intrinsic rotational correlation times of less than a few tenths of a nanosecond in aqueous solution. When covalently bound or adsorbed at the surface of a macromolecule, such a probe is thus expected to exhibit similarly rapid but restricted rotational diffusion around the bonds linking it to the macromolecule. The protein backbone is not rigid either, and local segmental flexibility of the polypeptide chain at the binding site, as well as "breathing motions" of protein subdomains, are also likely to contribute to the overall probe wobble. Correlation times for motions of these larger regions will more closely match the nanosecond lifetime of the excited state (Burghardt and Thompson, 1985; Van der Heide et al., 1992a).

The distinct time scales of the fast motions of the probe relative to the protein and the slower motions of the protein itself provide the rationale for the present analysis. It is strictly applicable only when all of the local restricted motions of the probe are much faster than its excited-state decay and the longer time-scale protein motions are much slower than this decay. Definitive characterization of the time course of probe motions requires nanosecond time-resolved measurements of polarized intensities. If the local restricted motions of the probe are not sufficiently fast compared with its excited-state decay, the order parameters $\langle P_{2a}\rangle$ and $\langle P_{2e}\rangle$ (or $\langle P_{2d}\rangle$) will tend to be overestimated, and the order parameters $\langle P_2\rangle$ and $\langle P_4\rangle$ describing the static part of the distribution will be underestimated (see Eqs. 15 and 16). Different orientational distributions of the probe in the ground and excited states would lead to further systematic errors in the analysis if the motions of the probe are not sufficiently fast.

Rotational motions on longer time scales, out to the microsecond and millisecond region, may be measured using triplet-state techniques (see, e.g., Jovin et al., 1981). Motions on the nanosecond time scale, like probe wobble and localized protein segmental reorientation, are effectively instantaneous on the microsecond to millisecond time scale of the triplet-state lifetime. Assuming as above that these are cylindrically symmetrical about a fixed axis in the macromolecule, application of the present analysis to data from the longer lifetime probes would include these motions in $\langle P_{2a}\rangle$ and $\langle P_{2e}\rangle$.

Comparison with earlier work

The analysis presented here is consistent with an earlier treatment for oriented membrane systems in which fluorophores exhibited "fast and slow orientational fluctuations" (Vogel and Jähnig, 1985), although the results presented there were limited to the case of colinear a and e and expressed in a more complicated form for a specific experimental geometry applicable to membrane systems. Stein et al. (1990) subsequently adapted the treatment of Vogel and Jähnig to polarized phosphorescence experiments in oriented muscle fibers. The present analysis is also consistent with the "compound motion" model derived for membrane systems in a more general manner (Van der Heide et al., 1993; Van der Sijs et al., 1993) and with the general treatment for muscle fibers given by Van der Heide et al. (1994).

The model of fast restricted probe rotation used in many previous studies of muscle fibers (Stein et al., 1990; Allen et al., 1996; Berger et al., 1996; Irving et al., 1995; Ling et al., 1996; Hopkins et al., 1998) assumes that the transition dipole moments are distributed uniformly within a cone of half-angle δ. This model was originally developed for membrane probes (Kinosita et al., 1977). However, the dipole orientations may not be uniformly distributed within the accessible range, for instance, in the presence of a central restoring force. The model invoked here is more general, because it applies to any cylindrically symmetrical distribution. The relationship between δ for the wobble-in-a-cone model and $\langle P_{2d}\rangle$ is given by

$$\langle P_{2d}\rangle = \frac{\int_0^{\delta} P_2(\cos\beta_{cd})\sin\beta_{cd}\,d\beta_{cd}}{\int_0^{\delta}\sin\beta_{cd}\,d\beta_{cd}} = \frac{\frac{1}{2}\int_0^{\delta}(3\cos^2\beta_{cd}-1)\sin\beta_{cd}\,d\beta_{cd}}{\int_0^{\delta}\sin\beta_{cd}\,d\beta_{cd}} = \frac{1}{2}\cos\delta\,(1+\cos\delta) \quad (42)$$

(Kinosita et al., 1977), and correspondingly for $\langle P_{2a} \rangle$ and $\langle P_{2e} \rangle$.

Example of application to labeled muscle fibers

Hopkins et al. (1998) presented steady-state polarization ratios obtained from skeletal muscle fibers containing regulatory light chains labeled with the 5- or 6-isomer of iodoacetamidotetramethylrhodamine (IATR), and fitted specific models of the static orientational distribution and wobble of the probes to these polarization ratios. Table 1 of the present paper shows the order parameters $\langle P_2 \rangle$, $\langle P_4 \rangle$, and $\langle P_{2d} \rangle$ calculated from these polarization ratios for the 6-IATR isomer in two experimental conditions: active contraction and rigor.

Some insight into the orientational distributions of the probe can be gained directly from the order parameters, without the use of specific orientation models. For both active contraction and rigor, the $\langle P_2 \rangle$ is negative, indicating that the probe orientational distribution with respect to the fiber axis is biased toward angles greater than 54.7°. Both $\langle P_2 \rangle$ and $\langle P_4 \rangle$ are closer to zero in active contraction than in rigor, indicating decreased order of the probes during active contraction. The value of $\langle P_{2d} \rangle$ is similar in active contraction and rigor, and close to unity, indicating that the extent of wobble is small and relatively independent of the physiological state.

Interpretation of the order parameters $\langle P_2 \rangle$ and $\langle P_4 \rangle$

Only two order parameters, $\langle P_2 \rangle$ and $\langle P_4 \rangle$, in the Legendre polynomial expansion for the probe distribution function, $f(\beta_{Fc})$ (Eq. 1), are available from the polarized fluorescence intensity data considered here. Although, as indicated above, some insight into the features of the orientational distribution can be obtained directly from them, these two order parameters alone cannot give, in general, an accurate representation of the underlying orientational distribution (Zannoni, 1988). $\langle P_2 \rangle$ and $\langle P_4 \rangle$ are still preferable to the polarization ratios for comparison of orientational distributions in different experimental conditions, because they exhibit a linear dependence on the fraction of probes in a particular orientational distribution. Thus, for example, a 1:1 mixture of two orientational distributions would have $\langle P_2 \rangle$ and $\langle P_4 \rangle$ values equal to the mean of the corresponding values for the two component distributions.

$\langle P_2 \rangle$ and $\langle P_4 \rangle$ do fully constrain simple two-parameter model distributions, such as an equal probability between two limiting angles (Stein et al., 1990), a Gaussian distribution characterized by its width and peak angle (Allen et al., 1996; Ling et al., 1996), or a two-population ensemble in which a fraction of the probes are randomly oriented and the remainder have a unique axial angle—the helix-plus-isotropic model (Tregear and Mendelson, 1975; Mendelson and Morales, 1977). The polarization ratios obtained in muscle fibers to date can generally be fitted by these distributions, but the interpretation may then depend on the specific model chosen.

A more general approach is to use information theory to derive a "maximum entropy" distribution that is the broadest distribution compatible with the data (Kooyman et al., 1983; Zannoni, 1988; Van der Heide et al., 1998). Finally, if $\langle P_2 \rangle$ and $\langle P_4 \rangle$ can be measured for several probes with different known orientations in the protein coordinate frame, the orientational distribution of the tilt and twist of the protein itself can be determined with respect to the fiber axis (Hopkins et al., 1997; Sabido-David et al., 1997).

TABLE 1 Example polarization ratios and derived order parameters

	Rigor	*n*	Active	*n*
$Q_{\parallel}$	0.144 ± 0.014	4	0.286 ± 0.028	16
${}^{x}Q_{\perp}$	0.486 ± 0.012	4	0.425 ± 0.019	16
${}^{y}Q_{\perp}$	0.060 ± 0.017	5	0.003 ± 0.006	5
$\langle P_{2d} \rangle$	0.924 ± 0.027		0.905 ± 0.025	
$\langle P_2 \rangle$	−0.136 ± 0.008		−0.059 ± 0.013	
$\langle P_4 \rangle$	−0.084 ± 0.016		−0.069 ± 0.015	

Steady-state polarization ratios from Hopkins et al. (1998) and derived values of the order parameters $\langle P_{2d} \rangle$, $\langle P_2 \rangle$, and $\langle P_4 \rangle$ with propagated error estimates given as standard deviations. The values given above of the standard deviations for the *Q* ratios were erroneously presented as standard errors of the mean (SEMs) in table 2 of Hopkins et al. (1998).

APPENDIX A: EXPANSION OF ORDER PARAMETERS AND CORRELATION FUNCTIONS USING VECTOR ROTATION GEOMETRY

In this appendix, Eqs. 5 and 6 in the Theory section of the text are derived from Eq. 4 in terms of simple trigonometric functions under the assumptions listed in the Introduction. First, average order parameters, $\langle P_{2a} \rangle$ and $\langle P_{2e} \rangle$, for the rapid restricted reorientation of the transition dipole moments *a* and *e* about the fixed axis *c* are factored out of those for the orientations of *a* and *e* with respect to *E* and *E′*, which appear in Eq. 4 both separately, $\langle P_2(\cos \beta_{Ea}) \rangle$ and $\langle P_2(\cos \beta_{E'e}) \rangle$, and in the form of their correlation function, $\langle P_2(\cos \beta_{Ea}) P_2(\cos \beta_{E'e}) \rangle$. This factorization establishes Eq. 5. Next, the parameters describing the orientation of the electric vectors of exciting light, *E*, and observed emission, *E′*, with respect to the fiber axis, *F*, are separated from the order parameter describing the orientation of *c* with respect to *F*, yielding the first two terms on the right-hand side of Eq. 6. Finally, the correlation function that appears as the average of the product of the second-rank Legendre polynomials describing the orientation of *c* with respect to *E* and *E′* in Eq. 5, $\langle P_2(\cos \beta_{Ec}) P_2(\cos \beta_{E'c}) \rangle$, is likewise expanded to give the last three terms in Eq. 6.

The angles between the absorption transition dipole moment *a*, the axis *c*, which is fixed in the frame of an immobile protein (assumption 3 in the Introduction), and the electric vector of the exciting light *E* (Fig. 2) are related by the completion theorem:

$$\cos \beta_{Ea} = \cos \beta_{Ec} \cos \beta_{ca} + \sin \beta_{Ec} \sin \beta_{ca} \cos \eta_{Ea}. \quad \text{(A1)}$$

Cylindrical symmetry of the distribution of *a* about *c* (assumption 2 in the Introduction) corresponds to the condition that all azimuths η_{Ea} of *a* about *c* (see Fig. 2) are equally probable. Squaring Eq. A1, averaging over η_{Ea}, and expressing the result in the form of second-rank Legendre poly-

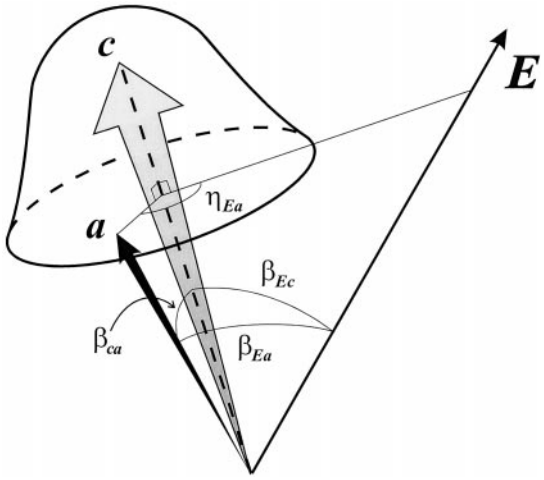

FIGURE 2 Geometrical relationship between the absorption transition dipole moment a of a fluorophore, the electric vector of exciting light E, and the axis c fixed in the labeled component. a is assumed to take up random azimuths η_{Ea} with respect to E about c, and to have a distribution of polar angles β_{ca} about c, represented diagrammatically here by the bell-shaped outline centered on c.

nomials leads to

$$\begin{aligned}\langle P_2(\cos\beta_{Ea})\rangle &= \frac{3}{2}\langle\cos^2\beta_{Ea}\rangle - \frac{1}{2}\\ &= \frac{9}{4}\langle\cos^2\beta_{Ec}\rangle\langle\cos^2\beta_{ca}\rangle - \frac{3}{4}\langle\cos^2\beta_{Ec}\rangle\\ &\quad - \frac{3}{4}\langle\cos^2\beta_{ca}\rangle + \frac{1}{4}\\ &= \langle P_2(\cos\beta_{ca})\rangle\langle P_2(\cos\beta_{Ec})\rangle\\ &= \langle P_{2a}\rangle\langle P_2(\cos\beta_{Ec})\rangle, \end{aligned} \tag{A2}$$

where $\langle\ \rangle$ explicitly signifies ensemble averaging over the azimuthal distribution of a with respect to c, and of c with respect to E, but also implicitly includes averaging over the distributions of β_{ca} and of β_{Ec}, respectively. This separation of the averages is justified by the independence of the orientational distribution of a about c from that of c in the system (assumption 2 in the Introduction). Application of the corresponding completion theorem relationship for e, c, and E',

$$\cos\theta_{E'e} = \cos\theta_{E'c}\cos\beta_{ce} + \sin\theta_{E'c}\sin\beta_{ce}\cos\eta_{E'e}, \tag{A3}$$

with averaging over the azimuth $\eta_{E'e}$, leads to the analogous result for the emission transition dipole moment:

$$\begin{aligned}\langle P_2(\cos\beta_{E'e})\rangle &= \langle P_2(\cos\beta_{ce})\rangle\langle P_2(\cos\beta_{E'c})\rangle\\ &= \langle P_{2e}\rangle\langle P_2(\cos\beta_{E'c})\rangle.\end{aligned} \tag{A4}$$

The correlation term $\langle P_2(\cos\beta_{Ea})P_2(\cos\beta_{E'e})\rangle$ in Eq. 4 is now considered. When the motion of e about c is very rapid (assumption 1 in the Introduction), its orientation within the restricted distribution about c becomes completely randomized before appreciable emission has occurred. Thus, within their respective distributions about c, the orientation of e at the moment of emission is independent of the orientation of a at the moment of excitation. Under this condition, $\langle P_{2a}\rangle$ and $\langle P_{2e}\rangle$ are mutually independent and can be factored out of the correlation term:

$$\begin{aligned}&\langle P_2(\cos\beta_{Ea})P_2(\cos\beta_{E'e})\rangle\\ &\quad = \langle P_{2a}\rangle\langle P_{2e}\rangle\langle P_2(\cos\beta_{Ec})P_2(\cos\beta_{E'c})\rangle.\end{aligned} \tag{A5}$$

Substitution of Eqs. A2, A4, and A5 into Eq. 4 in the Theory section leads to Eq. 5. Note that no restriction has yet been placed on the symmetry of the distributions of β_{Ec} and $\beta_{E'c}$.

If c is cylindrically symmetrical about the fiber axis F (assumption 4 in the Introduction), with azimuth η_{Ec} with respect to E and $\eta_{E'c}$ with respect to E', the expansions of the terms $\langle P_2(\cos\beta_{Ec})\rangle$ and $\langle P_2(\cos\beta_{E'c})\rangle$ in Eq. 5 follow from the completion theorem relationships:

$$\cos\beta_{Ec} = \cos\beta_{EF}\cos\beta_{Fc} + \sin\beta_{EF}\sin\beta_{Fc}\cos\eta_{Ec} \tag{A6}$$

$$\cos\beta_{E'c} = \cos\beta_{E'F}\cos\beta_{Fc} + \sin\beta_{E'F}\sin\beta_{Fc}\cos\eta_{E'c} \tag{A7}$$

in a manner analogous to those of $\langle P_2(\cos\beta_{Ea})\rangle$ and $\langle P_2(\cos\beta_{E'e})\rangle$ above, leading to

$$\langle P_2(\cos\beta_{Ec})\rangle = P_2(\cos\beta_{EF})\langle P_2(\cos\beta_{Fc})\rangle \tag{A8}$$

$$\langle P_2(\cos\beta_{E'c})\rangle = P_2(\cos\beta_{E'F})\langle P_2(\cos\beta_{Fc})\rangle, \tag{A9}$$

where again $\langle\ \rangle$ explicitly signifies averaging over the azimuths and includes implicit averaging over the distribution of β_{Fc}. The terms in β_{EF} and $\beta_{E'F}$ factor out of these averages, because they are constants of the geometrical set-up. Substitution of Eqs. A8 and A9 into Eq. 5 in the text gives rise to the terms in Eq. 6 containing S_a and S_e (defined in Eqs. 7 and 8).

It remains to expand the correlation function $\langle P_2(\cos\beta_{Ec})P_2(\cos\beta_{E'c})\rangle$ appearing in Eq. 5 to separate the geometrical factors relating E and E' to F from those relating c to F. Under the condition of cylindrical symmetry of c about F (assumption 4 in the Introduction), this involves averaging over the azimuths η_{Ec} and $\eta_{E'c}$, which are related by $\eta_{E'c} = \eta_{Ec} + \xi_{EE'}$, where $\xi_{EE'}$ is a constant of the geometry of excitation and observation (see Fig. 1). The completion theorem relationship for $\beta_{E'c}$ (Eq. A7) in terms of $\eta_{E'c} = \eta_{Ec} + \xi_{EE'}$ becomes

$$\begin{aligned}\cos\beta_{E'c} &= \cos\theta_{E'F}\cos\beta_{Fc} + \sin\theta_{E'F}\sin\beta_{Fc}\cos(\eta_{Ec} + \xi_{EE'})\\ &= \cos\theta_{E'F}\cos\beta_{Fc} + \sin\theta_{E'F}\sin\beta_{Fc}\\ &\quad (\cos\eta_{Ec}\cos\xi_{EE'} - \sin\eta_{Ec}\sin\xi_{EE'}).\end{aligned} \tag{A10}$$

Expansion of $\langle P_2(\cos\beta_{Ec})P_2(\cos\beta_{E'c})\rangle$ leads to

$$\begin{aligned}\langle P_2(\cos\beta_{Ec})P_2(\cos\beta_{E'c})\rangle &= \frac{9}{4}\langle\cos^2\beta_{Ec}\cos^2\beta_{E'c}\rangle\\ &\quad - \frac{3}{4}\langle\cos^2\beta_{Ec}\rangle - \frac{3}{4}\langle\cos^2\beta_{E'c}\rangle + \frac{1}{4},\end{aligned} \tag{A11}$$

in which the averages of $\cos^2\beta_{Ec}$ and $\cos^2\beta_{E'c}$ over η_{Ec} and $\eta_{E'c}$, respectively, are already implicit in Eqs. A8 and A9, the latter average also being obtainable by squaring Eq. A10 and averaging over η_{Ec}.

Substituting $\cos\beta_{Ec}$ and $\cos\beta_{E'c}$ from Eqs. A6 and A10 into $\langle\cos^2\beta_{Ec}\cos^2\beta_{E'c}\rangle$ in Eq. A11, multiplying out the product, and averaging over η_{Ec} leads to terms whose $\xi_{EE'}$ dependence can be expressed as cosines of integer multiples of $\xi_{EE'}$ (noting that $\cos 2\xi_{EE'} = 2\cos^2\xi_{EE'} - 1$) and $\xi_{EE'}$-independent terms. The latter, together with the remainder of the terms on the right-hand side of Eq. A11, can then be reexpressed via cosine powers and factored into β_{EF}-, $\beta_{E'F}$-, and β_{Fc}-dependent terms, leading

finally to

$$\langle P_2(\cos\beta_{Ec})P_2(\cos\beta_{E'c})\rangle = \left(\frac{3}{2}\cos^2\beta_{EF} - \frac{1}{2}\right)\left(\frac{3}{2}\cos^2\beta_{E'F} - \frac{1}{2}\right) \cdot \left\langle\left(\frac{3}{2}\cos^2\beta_{Fc} - \frac{1}{2}\right)^2\right\rangle + \frac{9}{2}(\cos\theta_{EF}\sin\theta_{EF}) \cdot (\cos\theta_{E'F}\sin\theta_{E'F})\cos\xi_{EE'}\langle\cos^2\beta_{Fc}\sin^2\beta_{Fc}\rangle + \frac{9}{32}\sin^2\theta_{EF}\sin^2\theta_{E'F}\cos 2\xi_{EE'}\langle\sin^4\beta_{Fc}\rangle. \quad \text{(A12)}$$

Substitution of Eq. A12 into Eq. A5 and of the result into Eq. 5 in the Theory section completes the derivation of Eq. 6, accounting for its last three terms containing G_0, G_1, and G_2 as defined in Eqs. 9–11.

APPENDIX B: WIGNER ROTATION MATRIX DERIVATIONS

In this Appendix we derive Eqs. 5 and 6 in the Theory section, using the Wigner rotation matrix formalism. In Eq. 5, rapid motions of the probes relative to the protein are factored out of the terms describing the protein orientation distribution. In Eq. 6, the factors describing the experimental geometry are separated from the order parameters and correlation functions S_a, S_e, G_0, G_1, and G_2 (Eqs. 7–11 in the text), which contain all of the information available from steady-state polarized fluorescence intensities about the orientational distribution and rotational motions of the probe molecules in the sample (Kooyman et al., 1981; Van Gurp et al., 1988b).

In these derivations, we use the elements $D^L_{m,n}(\alpha, \beta, \gamma)$ of the Wigner rotation matrix D^L. These elements form a set of functions that are conveniently used to rotate a frame through the three Euler angles α, β, and γ. An orientational distribution function can be expressed as a series expansion of the Wigner matrix elements because they form a complete set of orthogonal functions. These are defined here, according to the convention of Rose (1957), as

$$D^L_{m,n}(\alpha, \beta, \gamma) = e^{-im\alpha}d^L_{m,n}(\beta)e^{-in\gamma} \quad \text{(B1)}$$

with the small Wigner functions $d^L_{m,n}(\beta)$ given by

$$d^L_{m,n}(\beta) = \sum_{p=0}^{\infty}\left((-1)^p\frac{\sqrt{(L+m)!(L-m)!(L+n)!(L-n)!}}{(L-m-p)!(L+n-p)!(m-n+p)!p!} \cdot \left[\cos\left(\frac{\beta}{2}\right)\right]^{2L-m+n-2p}\left[-\sin\left(\frac{\beta}{2}\right)\right]^{m-n+2p}\right). \quad \text{(B2)}$$

In the above definition, the factorial of a negative number is taken to be infinite, so the summation will have a limited number of nonzero terms (at most $L + 1$ such terms for $L > 0$). From Eqs. B1 and B2, it can be shown that

$$D^L_{0,0}(\beta) \equiv d^L_{0,0}(\beta) = P_L(\cos\beta), \quad \text{(B3)}$$

which form the set of Legendre polynomials (see the definitions after Eq. 1 in the text). The other small Wigner functions used in this Appendix are

$$d^2_{1,0}(\beta) = -d^2_{0,1}(\beta) = d^2_{0,-1}(\beta) = -d^2_{-1,0}(\beta) = -\sqrt{\frac{3}{2}}\sin(\beta)\cos(\beta) \quad \text{(B4)}$$

$$d^2_{2,0}(\beta) = d^2_{0,2}(\beta) = d^2_{0,-2}(\beta) = d^2_{-2,0}(\beta) = \frac{1}{2}\sqrt{\frac{3}{2}}\sin^2(\beta). \quad \text{(B5)}$$

For a general configuration of linearly polarized excitation and fluorescence detection as defined in the text and in Fig. 1, the observed intensity is given by

$${}_EI_{E'} = \frac{I}{9}[1 + 2\langle P_2(\cos\beta_{Ea})\rangle + 2\langle P_2(\cos\beta_{E'e})\rangle + 4\langle P_2(\cos\beta_{Ea})P_2(\cos\beta_{E'e})\rangle], \quad \text{(B6)}$$

which is Eq. 4 in the text. First we modify Eq. B6 to separate terms that describe motions of the probe relative to an axis c, fixed in the protein, from those describing the orientation of c relative to the electric vectors of excitation and emission, E and E', respectively (Fig. 1). To this end, the rotations from E and E' to the transition dipole moments a and e, respectively, are resolved into two consecutive rotations: first from the direction of the electric vector to the frame connected with c (α_{Ec}, β_{Ec}, γ_{Ec}) for the excitation and similarly ($\alpha_{E'c}$, $\beta_{E'c}$, $\gamma_{E'c}$) for the emission, and then of the c-frame to that connected with the absorption dipole moment (α_{ca}, β_{ca}, γ_{ca}) or with the emission dipole moment (α_{ce}, β_{ce}, γ_{ce}), respectively. The rotation (α_{Ec}, β_{Ec}, γ_{Ec}), for instance, thus specifies the orientation of c with respect to E. The overall rotations are expressed in terms of these consecutive rotations by applying the closure relation for elements of the Wigner rotation matrices:

$$D^L_{m,n}(\alpha_{Ea}, \beta_{Ea}, \gamma_{Ea}) = \sum_{j=-L}^{L} D^L_{m,j}(\alpha_{Ec}, \beta_{Ec}, \gamma_{Ec})D^L_{j,n}(\alpha_{ca}, \beta_{ca}, \gamma_{ca}) \quad \text{(B7)}$$

$$D^L_{m,n}(\alpha_{E'e}, \beta_{E'e}, \gamma_{E'e}) = \sum_{k=-L}^{L} D^L_{m,k}(\alpha_{E'c}, \beta_{E'c}, \gamma_{E'c})D^L_{k,n}(\alpha_{ce}, \beta_{ce}, \gamma_{ce}) \quad \text{(B8)}$$

(Rose, 1957; Zannoni et al., 1983; Van der Heide et al., 1994). The ensemble averages of the second-rank Legendre polynomials and their product in Eq. B6 then become

$$\langle P_2(\cos\beta_{Ea})\rangle = \langle D^2_{0,0}(\beta_{Ea})\rangle = \sum_{j=-2}^{2}\langle D^2_{0,j}(\beta_{Ec}, \gamma_{Ec})D^2_{j,0}(\alpha_{ca}, \beta_{ca})\rangle \quad \text{(B9)}$$

$$\langle P_2(\cos\beta_{E'e})\rangle = \langle D^2_{0,0}(\beta_{E'e})\rangle = \sum_{k=-2}^{2}\langle D^2_{0,k}(\beta_{E'c}, \gamma_{E'c})D^2_{k,0}(\alpha_{ce}, \beta_{ce})\rangle \quad \text{(B10)}$$

$$\langle P_2(\cos\beta_{Ea})P_2(\cos\beta_{E'e})\rangle = \langle D^2_{0,0}(\beta_{Ea})D^2_{0,0}(\beta_{E'e})\rangle = \sum_{j=-2}^{2}\sum_{k=-2}^{2}\langle D^2_{0,j}(\beta_{Ec}, \gamma_{Ec})D^2_{j,0}(\alpha_{ca}, \beta_{ca}) \cdot D^2_{0,k}(\beta_{E'c}, \gamma_{E'c})D^2_{k,0}(\alpha_{ce}, \beta_{ce})\rangle. \quad \text{(B11)}$$

Assuming that the orientational distributions of *a* and *e* with respect to *c* are independent of the orientation of the protein (second part of assumption 2 in the Introduction), the ensemble averages on the right-hand sides of Eqs. B9–B11 are each equal to the product of two separate ensemble averages (Szabo, 1980):

$$\langle P_2(\cos\beta_{Ea})\rangle = \sum_{j=-2}^{2}\langle D^2_{0,j}(\beta_{Ec},\gamma_{Ec})\rangle\langle D^2_{j,0}(\alpha_{ca},\beta_{ca})\rangle \quad \text{(B12)}$$

$$\langle P_2(\cos\beta_{E'e})\rangle = \sum_{k=-2}^{2}\langle D^2_{0,k}(\beta_{E'c},\gamma_{E'c})\rangle\langle D^2_{k,0}(\alpha_{ce},\beta_{ce})\rangle \quad \text{(B13)}$$

$$\langle P_2(\cos\beta_{Ea})P_2(\cos\beta_{E'e})\rangle = \sum_{j=-2}^{2}\sum_{k=-2}^{2}\langle D^2_{0,j}(\beta_{Ec},\gamma_{Ec})D^2_{0,k}(\beta_{E'c},\gamma_{E'c})\rangle \cdot\langle D^2_{j,0}(\alpha_{ca(0)},\beta_{ca(0)})D^2_{k,0}(\alpha_{ce(t)},\beta_{ce(t)})\rangle. \quad \text{(B14)}$$

The last ensemble average in Eq. B14 represents the correlation between the orientation of *a* at the moment of excitation ($t = 0$) and *e* at the moment of emission, *t*. Therefore this ensemble average is sensitive to the motion of *e* before emission. At the instant of excitation, *a* and *e* are correlated (even if they are not colinear). When rotational relaxation is complete, then all "memory" of the orientation (within its restricted range) at the moment of excitation is lost. Thus the orientation of *e*, within its restricted range, at $t = \infty$, is independent of the orientation of *a*, within its restricted range, at excitation. This ensemble average then simplifies to

$$\sum_{j=-2}^{2}\sum_{k=-2}^{2}\langle D^2_{j,0}(\alpha_{ca(0)},\beta_{ca(0)})D^2_{k,0}(\alpha_{ce(t=\infty)},\beta_{ce(t=\infty)})\rangle = \sum_{j=-2}^{2}\langle D^2_{j,0}(\alpha_{ca},\beta_{ca})\rangle\sum_{k=-2}^{2}\langle D^2_{k,0}(\alpha_{ce},\beta_{ce})\rangle \quad \text{(B15)}$$

(Szabo, 1980; Zannoni et al., 1983).

If the rotation of the probe, and therefore the loss of correlation between *a* at the moment of excitation and *e* at the moment of emission, is very fast compared to the decay of the excited state (assumption 1) in the Introduction), then the time-dependent portion of Eq. B14 is negligible, and it is justified to use Eq. B15 as an approximation of the last ensemble average in Eq. B14.

So far we have not imposed any restrictions on the symmetry of the distribution of *a* and *e* relative to *c*. Assuming now that the distributions of *a* and *e* are cylindrically symmetrical about *c* (assumption 2 in the Introduction), the averages of $\exp(-ij\alpha_{ca})$ and $\exp(-ik\alpha_{ce})$ implied in Eqs. B12–B15 are nonzero only for *j* and *k* equal to zero. Then

$$\langle P_2(\cos\beta_{Ea})\rangle = \langle D^2_{0,0}(\beta_{ca})\rangle\langle D^2_{0,0}(\beta_{Ec})\rangle \quad \text{(B16)}$$

$$\langle P_2(\cos\beta_{E'e})\rangle = \langle D^2_{0,0}(\beta_{ce})\rangle\langle D^2_{0,0}(\beta_{E'c})\rangle \quad \text{(B17)}$$

$$\langle P_2(\cos\beta_{Ea})P_2(\cos\beta_{E'e})\rangle = \langle D^2_{0,0}(\beta_{ca})\rangle\langle D^2_{0,0}(\beta_{ce})\rangle\langle D^2_{0,0}(\beta_{Ec})D^2_{0,0}(\beta_{E'c})\rangle, \quad \text{(B18)}$$

in which the $t = \infty$ simplification of Eq. B15 is included. Replacing these Wigner functions with their equivalent Legendre polynomial forms, using the definitions $\langle P_{2a}\rangle = \langle P_2(\cos\beta_{ca})\rangle$ and $\langle P_{2e}\rangle = \langle P_2(\cos\beta_{ce})\rangle$, and substituting into Eq. B6 leads to

$${}_EI_{E'} = \frac{I}{9}[1 + 2\langle P_{2a}\rangle\langle P_2(\cos\beta_{Ec})\rangle + 2\langle P_{2e}\rangle\langle P_2(\cos\beta_{E'c})\rangle + 4\langle P_{2a}\rangle\langle P_{2e}\rangle\langle P_2(\cos\beta_{Ec})P_2(\cos\beta_{E'c})\rangle], \quad \text{(B19)}$$

which is Eq. 5 in the text.

Equation B19 separates the effects of rapid motion of the probe relative to *c* from the parameters describing the orientational distribution of *c* relative to *E* and *E*′. Next the latter must be expanded to separate the parts describing the experimental geometry from those describing the orientation of *c* relative to the fiber axis *F*. To this end, we express the rotation from each of the electric vectors *E* and *E*′ to *c* into two consecutive rotations, first from *E* or *E*′ to *F*, and then from *F* to *c*. This separation is again expressed in terms of the Wigner rotation matrices by applying the closure relation (cf. Eqs. B7 and B8):

$$\langle P_2(\cos\beta_{Ec})\rangle = \langle D^2_{0,0}(\beta_{Ec})\rangle = \sum_{j=-2}^{2}\langle D^2_{0,j}(\theta_{EF},\phi_{EF})D^2_{j,0}(\alpha_{Fc},\beta_{Fc})\rangle \quad \text{(B20)}$$

$$\langle P_2(\cos\beta_{E'c})\rangle = \langle D^2_{0,0}(\beta_{E'c})\rangle = \sum_{k=-2}^{2}\langle D^2_{0,k}(\theta_{E'F},\phi_{E'F})D^2_{k,0}(\alpha_{Fc},\beta_{Fc})\rangle \quad \text{(B21)}$$

$$\langle P_2(\cos\beta_{Ec})P_2(\cos\beta_{E'c})\rangle = \langle D^2_{0,0}(\beta_{Ec})D^2_{0,0}(\beta_{E'c})\rangle = \sum_{j=-2}^{2}\sum_{k=-2}^{2}\langle D^2_{0,j}(\theta_{EF},\phi_{EF})D^2_{j,0}(\alpha_{Fc},\beta_{Fc}) \cdot D^2_{0,k}(\theta_{E'F},\phi_{E'F})D^2_{k,0}(\alpha_{Fc},\beta_{Fc})\rangle, \quad \text{(B22)}$$

where (θ_{EF},ϕ_{EF}) and $(\theta_{E'F},\phi_{E'F})$ define the orientations of *E* and *E*′ in the *F* frame, ϕ_{EF} and $\phi_{E'F}$ being the azimuths formed by the projections of *E* and *E*′ onto the *xy* plane perpendicular to *F* (see Fig. 1). The dihedral angle between these projections is $\xi_{EE'} = \phi_{E'F} - \phi_{EF}$. Because the orientations of *E* and *E*′ relative to *F* are fixed, the *EF*- and *E*′*F*-dependent parameters can be removed from the ensemble averages, giving

$$\langle P_2(\cos\beta_{Ec})\rangle = \sum_{j=-2}^{2}D^2_{0,j}(\theta_{EF},\phi_{EF})\langle D^2_{j,0}(\alpha_{Fc},\beta_{Fc})\rangle \quad \text{(B23)}$$

$$\langle P_2(\cos\beta_{E'c})\rangle = \sum_{k=-2}^{2}D^2_{0,k}(\theta_{E'F},\phi_{E'F})\langle D^2_{k,0}(\alpha_{Fc},\beta_{Fc})\rangle \quad \text{(B24)}$$

$$\langle P_2(\cos\beta_{Ec})P_2(\cos\beta_{E'c})\rangle = \sum_{j=-2}^{2}\sum_{k=-2}^{2}D^2_{0,j}(\theta_{EF},\phi_{EF})D^2_{0,k}(\theta_{E'F},\phi_{E'F}) \cdot\langle D^2_{j,0}(\alpha_{Fc},\beta_{Fc})D^2_{k,0}(\alpha_{Fc},\beta_{Fc})\rangle. \quad \text{(B25)}$$

If the orientational distribution of the protein in the fiber is cylindrically symmetrical about F (assumption 4 in the Introduction), only the terms with j and k zero, respectively in Eqs. B22 and B23, survive, leading to

$$\langle P_2(\cos\beta_{Ec})\rangle = D^2_{0,0}(\theta_{EF})\langle D^2_{0,0}(\beta_{Fc})\rangle \quad \text{(B26)}$$

$$\langle P_2(\cos\beta_{E'c})\rangle = D^2_{0,0}(\theta_{E'F})\langle D^2_{0,0}(\beta_{Fc})\rangle. \quad \text{(B27)}$$

In the average of the product $\exp(-i(j + k)\alpha_{Fc})$ implied in Eq. B25, only those terms for which $j = -k$ survive. Thus,

$$\langle P_2(\cos\beta_{Ec})P_2(\cos\beta_{E'c})\rangle = \sum_{j=-2}^{2} D^2_{0,j}(\theta_{EF}, \phi_{EF})D^2_{0,-j}(\theta_{E'F}, \phi_{E'F}) \cdot \langle D^2_{j,0}(\alpha_{Fc}, \beta_{Fc})D^2_{-j,0}(\alpha_{Fc}, \beta_{Fc})\rangle. \quad \text{(B28)}$$

We can now use the identities given in Eqs. B1–B5 to rewrite Eqs. B26–B28 as

$$\langle P_2(\cos\beta_{Ec})\rangle = \left(\frac{3}{2}\cos^2\theta_{EF} - \frac{1}{2}\right)\left\langle\left(\frac{3}{2}\cos^2\beta_{Fc} - \frac{1}{2}\right)\right\rangle \quad \text{(B29)}$$

$$\langle P_2(\cos\beta_{E'c})\rangle = \left(\frac{3}{2}\cos^2\theta_{E'F} - \frac{1}{2}\right)\left\langle\left(\frac{3}{2}\cos^2\beta_{Fc} - \frac{1}{2}\right)\right\rangle \quad \text{(B30)}$$

$$\begin{aligned}\langle P_2(\cos\beta_{Ec})P_2(\cos\beta_{E'c})\rangle &= \left(\frac{3}{2}\cos^2\theta_{EF} - \frac{1}{2}\right)\left(\frac{3}{2}\cos^2\theta_{E'F} - \frac{1}{2}\right)\\ &\cdot\left\langle\left(\frac{3}{2}\cos^2\beta_{Fc} - \frac{1}{2}\right)^2\right\rangle + \frac{9}{2}(\cos\theta_{EF}\sin\theta_{EF})\\ &\cdot(\cos\theta_{E'F}\sin\theta_{E'F})\cos(\phi_{E'F} - \phi_{EF})\langle\cos^2\beta_{Fc}\sin^2\beta_{Fc}\rangle\\ &+ \frac{9}{32}\sin^2\theta_{EF}\sin^2\theta_{E'F}\cos 2(\phi_{E'F} - \phi_{EF})\langle\sin^4\beta_{Fc}\rangle.\end{aligned} \quad \text{(B31)}$$

Insertion of Eqs. B29–B31 into Eq. B18, together with the identity $\xi_{EE'} = \phi_{E'F} - \phi_{EF}$ indicated above, yields Eq. 6 in the main text with the definitions in Eqs. 7–11.

We thank Drs. Joseph N. Forkey and Henry Shuman for useful discussions. This work was supported by National Institutes of Health grant AR26846, the Muscular Dystrophy Associations of America (YEG), the American Heart Association (SCH), The Wellcome Trust, U.K. (RED, TM, and MI), and the Polish Government through KBN grant 2 PO3B 12409 (TM).

REFERENCES

Allen, T. St. C., N. Ling, M. Irving, and Y. E. Goldman. 1996. Orientation changes in myosin regulatory light chains following photorelease of ATP in skinned muscle fibers. *Biophys. J.* 70:1847–1862.

Badea, M. G., and L. Brand. 1979. Time-resolved fluorescence measurements. *Methods Enzymol.* 61:378–425.

Beechem, J. M., and L. Brand. 1985. Time-resolved fluorescence of proteins. *Annu. Rev. Biochem.* 54:43–71.

Berger, C. L., J. S. Craik, D. R. Trentham, J. E. T. Corrie, and Y. E. Goldman. 1996. Fluorescence polarization of skeletal muscle fibers labeled with rhodamine isomers on the myosin heavy chain. *Biophys. J.* 71: 3330–3343.

Brochon, J.-C., Ph. Wahl, and J. C. Auchet. 1972. Mesure des déclins de l'anisotropie de fluorescence de la γ-globuline et de ses fragments Fab, Fc et $F(ab)_2$ marqués avec le 1-sulfonyl-5-diméthyl-aminonaphtalène. *Eur. J. Biochem.* 25:20–32.

Burghardt, T. P., and N. L. Thompson. 1985. Motion of myosin cross-bridges in skeletal muscle fibers studied by time-resolved fluorescence anisotropy decay. *Biochemistry.* 24:3731–3735.

Chen, R. F., and R. L. Bowman. 1965. Fluorescence polarization: measurement with ultraviolet-polarizing filters in a spectrophotofluorometer. *Science.* 147:729–732.

Dale, R. E., T. Marszalek, S. C. Hopkins, M. Irving, and Y. E. Goldman. 1997. Model-independent analysis of mobility and orientation of fluorescent probes in muscle fibers. *Biophys. J.* 72:A52.

Hopkins, S. C., C. Sabido-David, B. D. Brandmeier, J. Kendrick-Jones, R. E. Dale, J. E. T. Corrie, D. R. Trentham, M. Irving, and Y. E. Goldman. 1997. Motions of bifunctional rhodamine probes with defined orientations on the regulatory light chain (RLC) in skeletal muscle fibers. *Biophys. J.* 72:A1.

Hopkins, S. C., C. Sabido-David, J. E. T. Corrie, M. Irving, and Y. E. Goldman. 1998. Fluorescence polarization transients from rhodamine isomers on the myosin regulatory light chain in skeletal muscle fibers. *Biophys. J.* 74:3093–3110.

Irving, M. 1996. Steady-state polarization from cylindrically symmetric fluorophores undergoing rapid restricted motion. *Biophys. J.* 70: 1830–1835.

Irving, M., T. St. C. Allen, C. Sabido-David, J. S. Craik, B. Brandmeier, J. Kendrick-Jones, J. E. T. Corrie, D. R. Trentham, and Y. E. Goldman. 1995. Tilting of the light-chain region of myosin during step length changes and active force generation in skeletal muscle. *Nature.* 375: 688–691.

Ishiwata, S., K. Kinosita, Jr., H. Yoshimura, and A. Ikegami. 1987. Rotational motions of myosin heads in myofibril studied by phosphorescence anisotropy decay measurements. *J. Biol. Chem.* 262: 8314–8317.

Johansson, L. B.-Å. 1985. Order parameters of fluorophores in ground and excited states. Probe molecules in a lyotropic liquid crystal. *Chem. Phys. Lett.* 118:516–521.

Jovin, T. M., M. Bartholdi, W. L. C. Vaz, and R. H. Austin. 1981. Rotational diffusion of biological macromolecules by time-resolved delayed luminescence (phosphorescence, fluorescence) anisotropy. *Ann. N.Y. Acad. Sci.* 366:176–196.

Kinosita, K., Jr., S. Ishiwata, H. Yoshimura, H. Asai, and A. Ikegami. 1984. Submicrosecond and microsecond rotational motions of myosin head in solution and in myosin synthetic filaments as revealed by time-resolved optical anisotropy decay measurements. *Biochemistry.* 23:5963–5975.

Kinosita, K., Jr., S. Kawato, and A. Ikegami. 1977. A theory of fluorescence polarization decay in membranes. *Biophys. J.* 20:289–305.

Kooyman, R. P. H., Y. K. Levine, and B. W. van der Meer. 1981. Measurement of second and fourth rank order parameters by fluorescence polarization experiments in a lipid membrane system. *Chem. Phys.* 60:317–326.

Kooyman, R. P. H., M. H. Vos, and Y. K. Levine. 1983. Determination of orientational order parameters in oriented lipid membrane systems by angle-resolved fluorescence depolarization experiments. *Chem. Phys.* 81:461–472.

Lakowicz, J. R. 1983. Principles of Fluorescence Spectroscopy. Plenum Press, New York.

Lakowicz, J. R., and B. P. Maliwal. 1985. Construction and performance of a variable-frequency phase-modulation fluorometer. *Biophys. Chem.* 21:61–78.

Ling, N., C. Shrimpton, J. Sleep, J. Kendrick-Jones, and M. Irving. 1996. Fluorescent probes of the orientation of myosin regulatory light chains in relaxed, rigor, and contracting muscle. *Biophys. J.* 70:1836–1846.

Ludescher, R. D., and D. D. Thomas. 1988. Microsecond rotational dynamics of phosphorescent-labeled muscle cross-bridges. *Biochemistry.* 27:3343–3351.

Mendelson, R. A., and M. F. Morales. 1977. Appendix in: Borejdo, J., and S. Putnam. Polarization of fluorescence from single skinned glycerinated rabbit psoas fibers in rigor and relaxation. *Biochim. Biophys. Acta.* 459:578–595.

Mendelson, R. A., M. F. Morales, and J. Botts. 1973. Segmental flexibility of the S-1 moiety of myosin. *Biochemistry.* 12:2250–2255.

Mulders, F., H. van Langen, G. van Ginkel, and Y. K. Levine. 1986. The static and dynamic behaviour of fluorescent probe molecules in lipid bilayers. *Biochim. Biophys. Acta.* 859:209–218.

Munro, I., I. Pecht, and L. Stryer. 1979. Subnanosecond motions of tryptophans in proteins. *Proc. Natl. Acad. Sci. USA.* 76:56–60.

Penzkofer, A., and J. Wiedmann. 1980. Orientation of transition dipole moments of rhodamine 6G determined by excited state absorption. *Optics Commun.* 35:81–86.

Razi Naqvi, K. 1981. Photoselection in uniaxial liquid crystals: the advantages of using saturating light pulses for the determination of orientational order. *J. Chem. Phys.* 74:2658–2659.

Rose, M. E. 1957. Elementary Theory of Angular Momentum. Wiley, New York.

Sabido-David, C., R. E. Ferguson, B. D. Brandmeier, S. C. Hopkins, Y. E. Goldman, J. Kendrick-Jones, R. E. Dale, J. E. T. Corrie, D. R. Trentham, and M. Irving. 1997. Orientation of bifunctional rhodamine probes on myosin regulatory light chain (RLC) in relaxed, contracting and rigor muscle. *Biophys. J.* 72:A52.

Stein, R. A., R. D. Ludescher, P. S. Dahlberg, P. G. Fajer, R. L. H. Bennett, and D. D. Thomas. 1990. Time-resolved rotational dynamics of phosphorescent-labeled myosin heads in contracting muscle fibers. *Biochemistry.* 29:10023–10031.

Szabo, A. 1980. Theory of polarized fluorescent emission in uniaxial liquid crystals. *J. Chem. Phys.* 72:4620–4626.

Tregear, R. T., and R. A. Mendelson. 1975. Polarization from a helix of fluorophores and its relation to that obtained from muscle. *Biophys. J.* 15:455–467.

Van der Heide, U. A., H. C. Gerritsen, I. P. Trayer, and Y. K. Levine. 1992a. Determination of the orientation of fluorescent labels relative to myosin S_1 in solution from time resolved fluorescence anisotropy experiments. *Proc. SPIE Int. Soc. Opt. Eng.* 1640:681–689.

Van der Heide, U. A., S. C. Hopkins, and Y. E. Goldman. 1998. A maximum entropy analysis of the orientation of regulatory light chains in skeletal muscle fibers. *Biophys. J.* 74:A364.

Van der Heide, U. A., B. Orbons, H. C. Gerritsen, and Y. K. Levine. 1992b. The orientation of transition moments of dye molecules used in fluorescence studies of muscle systems. *Eur. Biophys. J.* 21:263–272.

Van der Heide, U. A., O. E. Rem, H. C. Gerritsen, E. L. de Beer, P. Schiereck, I. P. Trayer, and Y. K. Levine. 1994. A fluorescence depolarization study of the orientational distribution of cross-bridges in muscle fibres. *Eur. Biophys. J.* 23:369–378.

Van der Heide, U. A., M. A. M. J. Zandvoort, E. van Faassen, G. van Ginkel, and Y. K. Levine. 1993. On the interpretation of fluorescence anisotropy decays from probe molecules in lipid vesicle systems. *J. Fluorescence.* 3:271–279.

Van der Meer, B. W., R. P. H. Kooyman, and Y. K. Levine. 1982. A theory of fluorescence depolarization in macroscopically ordered membrane systems. *Chem. Phys.* 66:39–50.

Van der Sijs, D. A., E. E. van Faassen, and Y. K. Levine. 1993. The interpretation of fluorescence anisotropy decays of probe molecules in membrane systems. *Chem. Phys. Lett.* 216:559–565.

Van Gurp, M., G. van Ginkel, and Y. K. Levine. 1988a. Orientational properties of biological pigments in ordered systems studied with polarized light: photosynthetic pigment-protein complexes in membranes. *J. Theoret. Biol.* 131:333–349.

Van Gurp, M., H. van Langen, G. van Ginkel, and Y. K. Levine. 1988b. Angle-resolved techniques in studies of organic molecules in ordered systems using polarized light. *In* Polarized Spectroscopy of Ordered Systems. B. Samori' and E. W. Thulstrup, editors. Kluwer Academic Publishers, Dordrecht. 455–489.

Vogel, H., and F. Jähnig. 1985. Fast and slow orientational fluctuations in membranes. *Proc. Natl. Acad. Sci. USA.* 82:2029–2033.

Wahl, P., K. Tawada, and J. C. Auchet. 1978. Study of tropomyosin labelled with a fluorescent probe by pulse fluorimetry in polarized light. Interaction of that protein with troponin and actin. *Eur. J. Biochem.* 88:421–424.

Yguerabide, J., H. F. Epstein, and L. Stryer. 1970. Segmental flexibility in an antibody molecule. *J. Mol. Biol.* 51:573–590.

Zannoni, C. 1988. Order parameters and orientational distributions in liquid crystals. *In* Polarized Spectroscopy of Ordered Systems. B. Samori' and E. W. Thulstrup, editors. Kluwer Academic Publishers, Dordrecht. 57–83.

Zannoni, C., A. Arcioni, and P. Cavatorta. 1983. Fluorescence depolarization in liquid crystals and membrane bilayers. *Chem. Phys. Lipids.* 32:179–250.